

Article

The Upwelling Groundwater Flow in the Karst Area of Grassano-Telese Springs (Southern Italy)

Francesco Fiorillo, Guido Leone, Mauro Pagnozzi *, Vittorio Catani, Giovanni Testa and Libera Esposito

Department of Science and Technology, University of Sannio, 82100 Benevento, Italy; francesco.fiorillo@unisannio.it (F.F.); guido.leone93@gmail.com (G.L.); vittoriocatani@gmail.com (V.C.); geologo.giannitesta@gmail.com (G.T.); libera.esposito@unisannio.it (L.E.)

* Correspondence: pagnozzi.mauro@libero.it; Tel.: +39-0824-305195

Received: 28 February 2019; Accepted: 22 April 2019; Published: 26 April 2019



Abstract: The hydraulic phenomenon of upwelling groundwater flow affecting the karst area of the Grassano-Telese springs (southern Italy) has been investigated through piezometric measurements, discharge, and chemical–physical monitoring of springs, radon activity included. Locally, both large karst springs and sulfurous thermal springs are closely located, and raise several questions on their origin. In this study, the phenomenon of the upwelling flow is supported by different types of evidences: Amazing density of sinkholes connected to hypogenic speleogenesis processes, constancy of temperature, and hydraulic conductivity of spring water, change of radon activity during the hydrological year, increasing of the hydraulic head with depth. Numerical code provides an estimation of the upwelling phenomenon in an unconfined aquifer feeding the karst springs, using MODFLOW tools. Based on the results reached, the phenomenon of the upwelling flow is able to explain the hydrological processes observed in the Telese karst area.

Keywords: karst springs; sulfurous springs; upwelling flux; hydraulic head; sinkholes; groundwater modeling; radon

1. Introduction

Karst systems are able to concentrate in a restricted zone, the discharge area, the drainage of a wide groundwater catchment [1–3]. In the discharge area, a single or a group of karst springs are located, which originate or feed rivers.

Karst aquifers can be characterized by a high transmissivity and a high capacity to store large volumes of water, which allow a deep-water circulation generating ascendant flows in the discharge zones, where basal springs are located [4].

The upwelling phenomenon that affects some basal karst springs can be associated to the regional groundwater model [5–7], in which descendant and ascendant flows characterize the recharge and discharge area, respectively. In particular, discharge areas are located in depressed zones, where rivers increase their discharge through linear or punctual springs. However, although flowrate and other physical and chemical features of springs can be easily measured, the ascendant flux is not easy to detect, due to a local vertical hydraulic gradient, which is difficult to recognize. Fiorillo et al. [4] highlight the upwelling flux phenomenon feeding the Serino springs, in southern Italy, based on piezometric data and the chemical–physical parameters of spring waters, providing three different hydrogeological sketches describing the ascendant flow of spring outlets (Figure 1). The upwelling phenomenon of groundwater is a consequence of artesian conditions (Figure 1a), but it can occur also in unconfined aquifers of wide karst systems (Figure 1b,c).

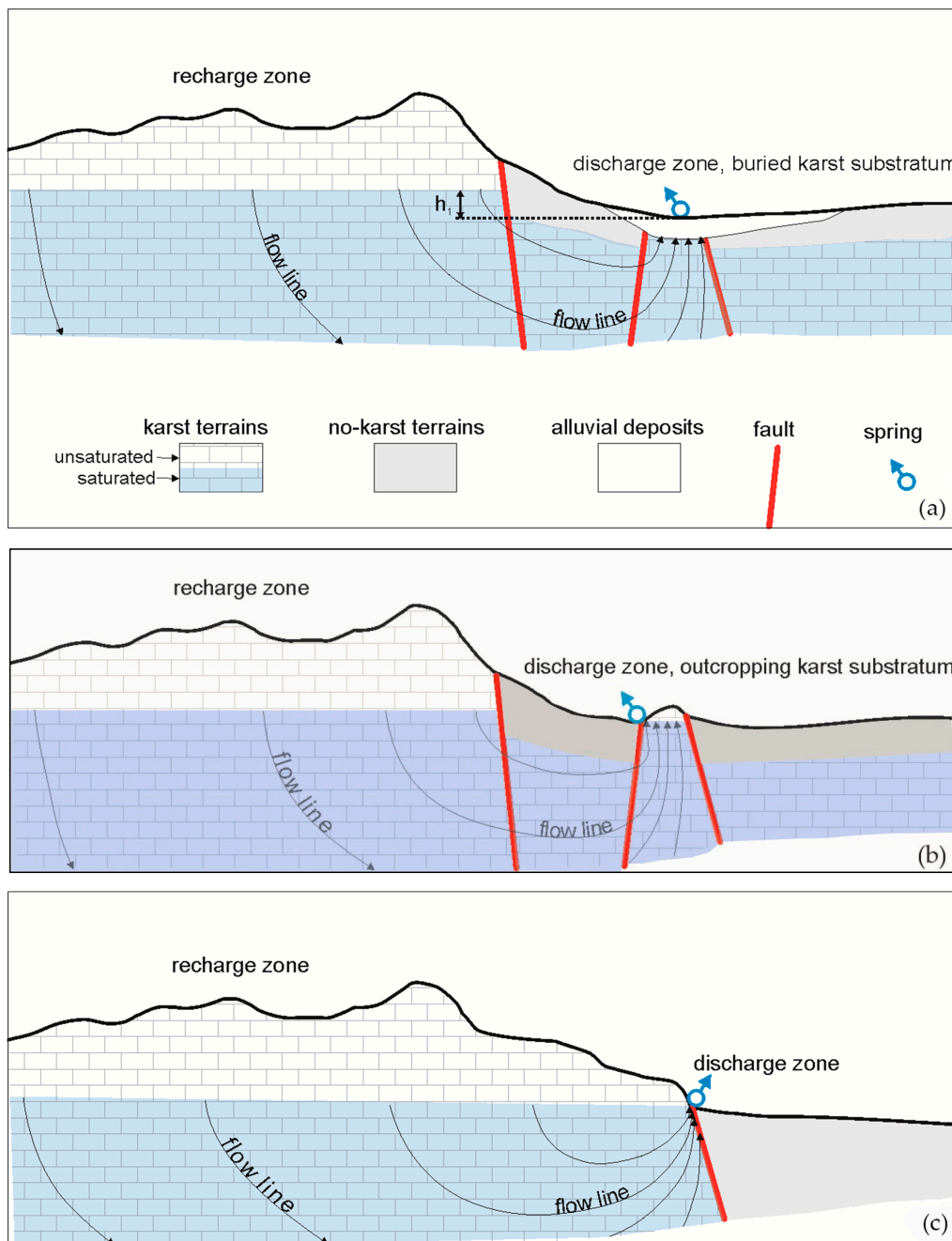


Figure 1. Ascendant flux connected to different hydrogeological settings of the discharge zone of karst aquifers (a) the hydraulic head difference, h_1 , is needed to allow the rising of groundwater through the porous medium from buried karst substratum; (b) no-karst terrains between the recharge and discharge area help groundwater syphoning; (c) flow lines tend to be vertical as a consequence of deep groundwater flow and flat water table (modified from Fiorillo et al. [4]).

In this study, specific hydrogeological surveys and computer modeling have been carried out for the Teles discharge area (southern Italy), where sulfurous thermal springs are close to large cold karst springs. Locally, the extraordinary density of sinkholes has been also considered.

The ascendant flow assessment is based on the analysis of hydraulic head monitoring, chemical, and physical data of spring water, including ^{222}Rn activity measurements. The groundwater flow has been modeled by MODFLOW computer tools, supporting the upwelling phenomenon in the Teles discharge area.

2. Materials and Methods

Methods used concern sinkhole mapping, chemical and physical characteristics of spring water, and numerical modeling of groundwater. Remotely sensed data and topographic maps have been used in order to map all the sinkholes and analyze their distribution and morphometry.

Major sinkhole upper-rim delineation was performed using geographical information systems (GIS) for the visual analysis of a hill shade model as well as contour maps derived from a high-resolution (1×1 m and 5×5 m cell) digital elevation model (DEM), and digital orthophotos with a resolution of 0.5 m. Instead, a field geological survey, combined with the analysis of detailed topographic maps, was necessary for the identification of both small and anthropized sinkholes.

Monthly measurements of the discharge, temperature, electrical conductivity (E.C.), and ^{222}Rn activity were carried out in the spring waters.

Discharge measurements have been carried out since 2014 through a hydrometric boat with an acoustic profiler Doppler, which can acquire riverbed velocity and section simultaneously.

Temperature and electrical conductivity data were acquired through a multiparametric probe (Horiba model U50), immersing the sensor in correspondence to the outlet springs; values have been compensated at 20 °C.

The ^{222}Rn activity measurements were carried out sampling spring waters. The samples, immediately sealed by parafilms, were transported to the Laboratory of Hydrogeology of the University of Sannio for measurements of ^{222}Rn activity with a minimum delay time from collection time (30'). Radon activity was performed using the AlphaGUARD radon detector (Genitron Instruments GmbH, Germany): A pulse-counting ionization chamber suitable for alpha spectroscopy. Samples of 100 mL of water were taken in glass bottles. Detected ^{222}Rn activity levels were analyzed using the software Data EXPERT (by GENITRON Instruments). The main interest of ^{222}Rn activity in spring waters is its possible connection with groundwater velocity and consequently its variation during the high or low flow conditions of the spring [4].

To model the groundwater flow, the PROCESSING MODFLOW numerical code [8,9] has been used to simulate the phenomenon of the upwelling flow, along a vertical section crossing the spring outlet and considering only one layer to model the aquifer. The numerical code of PROCESSING MODFLOW is based on the Dupuit approximation and finite difference method and its use is limited to modeling groundwater flow and solving the problem of transport processes in saturated systems.

The simulation was calibrated by the hydraulic head measurement upstream of the spring outlet, and provides the path of the flow and equipotential lines under specific hydraulic boundary conditions, using MODPATH tools [10,11]. In particular, in the IBOUND tools we chose “active cell” for karst aquifer, “no-flow zone” for flysch sequences, and distinguished aquitard from aquifer using a different hydraulic conductivity.

The aim is to simulate the groundwater flow paths and highlight the upwelling phenomenon under the spring, rather than to estimate the discharge amount.

3. Study Area

The Grassano and Telesse springs are believed to belong the wide karst area of the Matese massif [12–17]. The massif outcrops in the median sector of the Apennine chain (Figure 2) and it is characterized by high slopes and elevations up to 2050 m above sea level (hereafter m a.s.l.) of Mt. Miletto.

The rocks belong to a limestone and limestone–dolomite (late Triassic–Miocene) series, characterized by a thickness ranging between 2500 and 3000 m. Along the northern and eastern sectors, the massif is tectonically joined by a thrust fault to low permeability argillaceous complexes (Paleocene) and flysch sequences (Miocene). Along the southern and western sectors, the massif is bounded by normal faults and it is covered by recent quaternary deposits of the Volturno river plain. More specific geological insight of the outcropping areas can be found in Robustini et al. [18] and the Geological Map of Italy, scale 1:100,000 (<http://www.isprambiente.gov.it>).

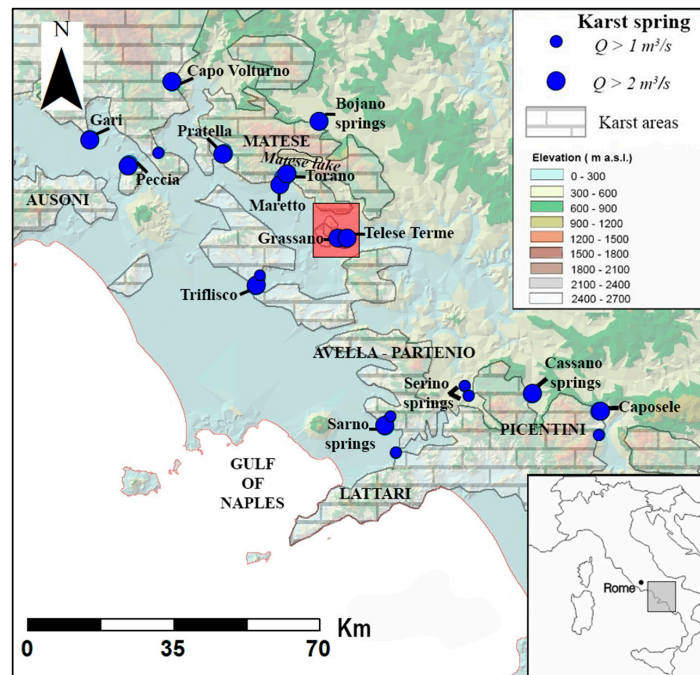


Figure 2. Hydrogeological overview of the western sector of Campania. Red rectangle shows the study area.

The Matese massif feeds many basal karst springs; the Grassano-Telesse springs are located in the extreme southeastern zone, along the southern side of the Montepugliano relief (Figure 3a–c). Many of these karst springs are connected to wide endorheic areas, which occupy the high elevations of the Matese massif, and play an important role in the recharge processes [17].

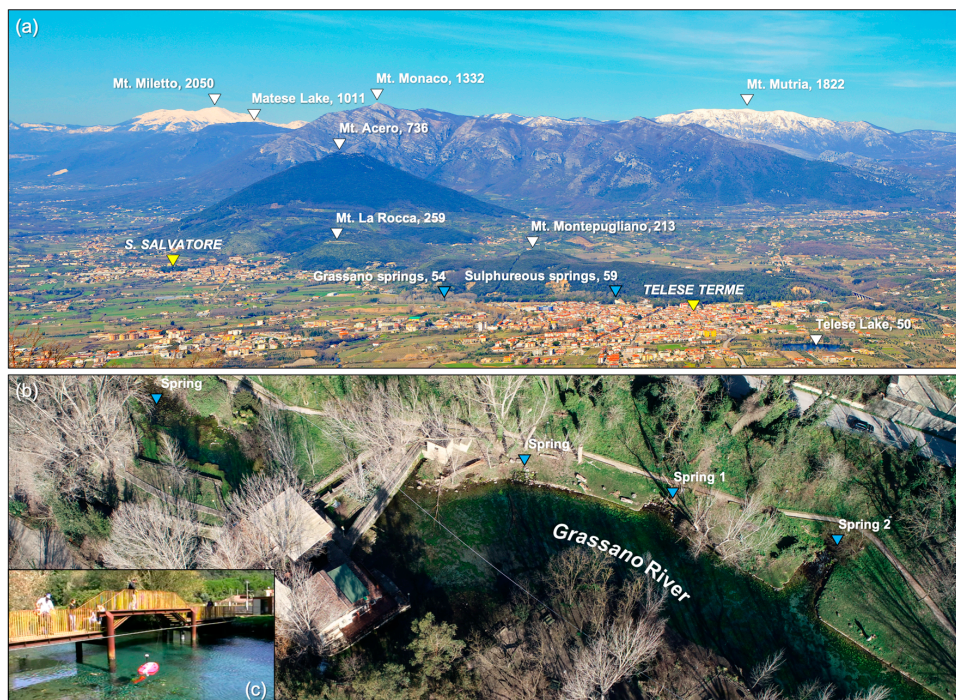


Figure 3. View of the southern side of the Matese massif (a) and location of the Grassano springs group (b). Discharge measurements of the springs have been carried out in correspondence of the bridge (c) using hydrometric boat with an acoustic profiler Doppler.

The main endorheic area is the Lago Matese polje, with an area of 45 km², located in the high-ground elevated sector of the massif, between 1000 and 2050 m a.s.l. Locally, a permanent lake exists, which was exploited for hydroelectrical purposes. During the beginning of the last century, hydraulic works have isolated the main sinkholes by earth dams and have tried to waterproof the bottom of the lake. Before these hydraulic works, the connection between Matese lake and Grassano-Telese springs was discussed by Gauthier [12], who described how provisional dams in the Matese lake influenced the regime of these springs also. Based on hydrogeological considerations, the entire eastern sector of the Matese massif has to be the main catchment of the Grassano-Telese springs [15]. This sector is hydraulically connected with the Grassano springs by buried karst terrains and outcropping karst reliefs as Mt. Monaco, Mt. Acero, and Montepugliano (Figure 4). Thus, the Montepugliano relief can be considered the discharge zone of a wide portion of the Matese massif, and it is characterized by an extraordinary density of sinkholes (Figure 5). As the Grassano springs are located at 54 m a.s.l., they constitute the lowest spring group of the entire Matese massif [17]; however, their hydraulic connection with the Matese massif is not easy to explain, also because karst terrains outcrop discontinuously along a narrow zone between the Montepugliano relief and Mt. Monaco (Figure 4). Besides, due to outcropping of the flysch sequences and the presence of the Titero river between the Montepugliano relief and Mt. Monaco, syphoning phenomena has to occur.

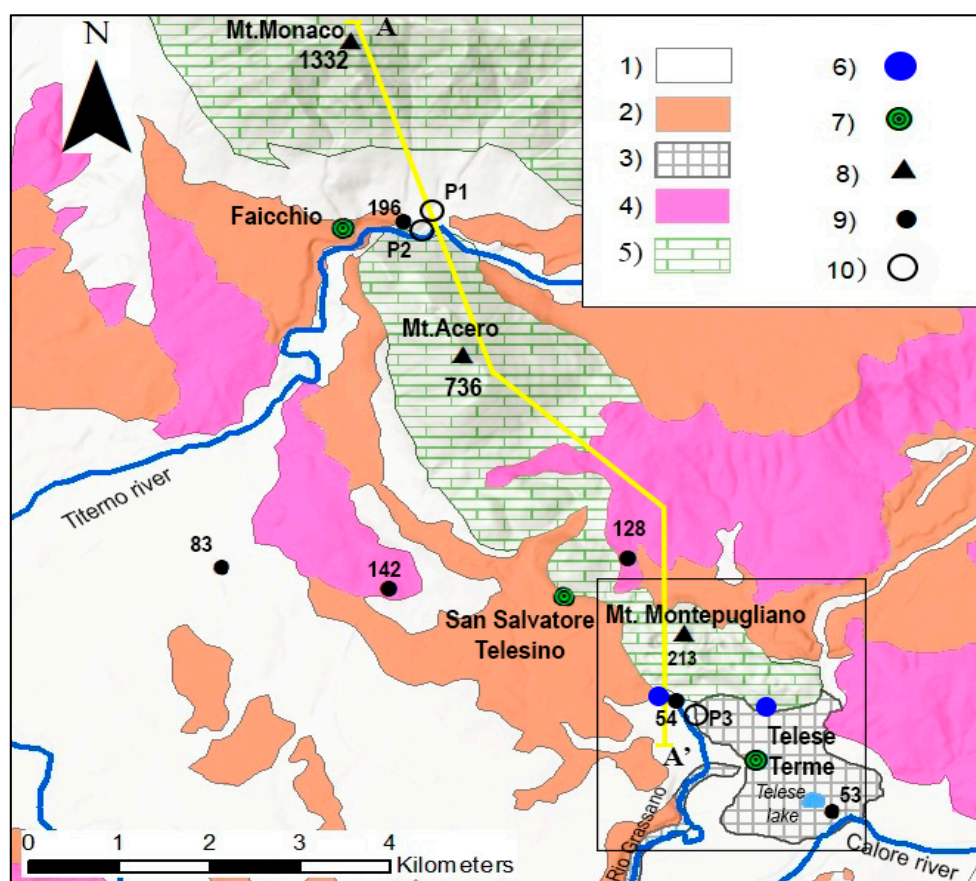


Figure 4. Overview of the Telese karst area: (1) Alluvial and lacustrine deposits of the Telese plain (Quaternary); (2) Campanian Ignimbrite and pyroclastic deposits (Quaternary); (3) travertine deposits (Quaternary); (4) argillaceous complex and flysch sequences (Paleogene–Miocene); (5) calcareous dolomite series (Jurassic–Miocene); (6) spring; (7) village; (8) mountain peak; (9) elevation (m a.s.l.); (10) borehole; yellow line is section trace AA' shown in Figure 9. The area marked with black rectangle is detailed in Figure 5.

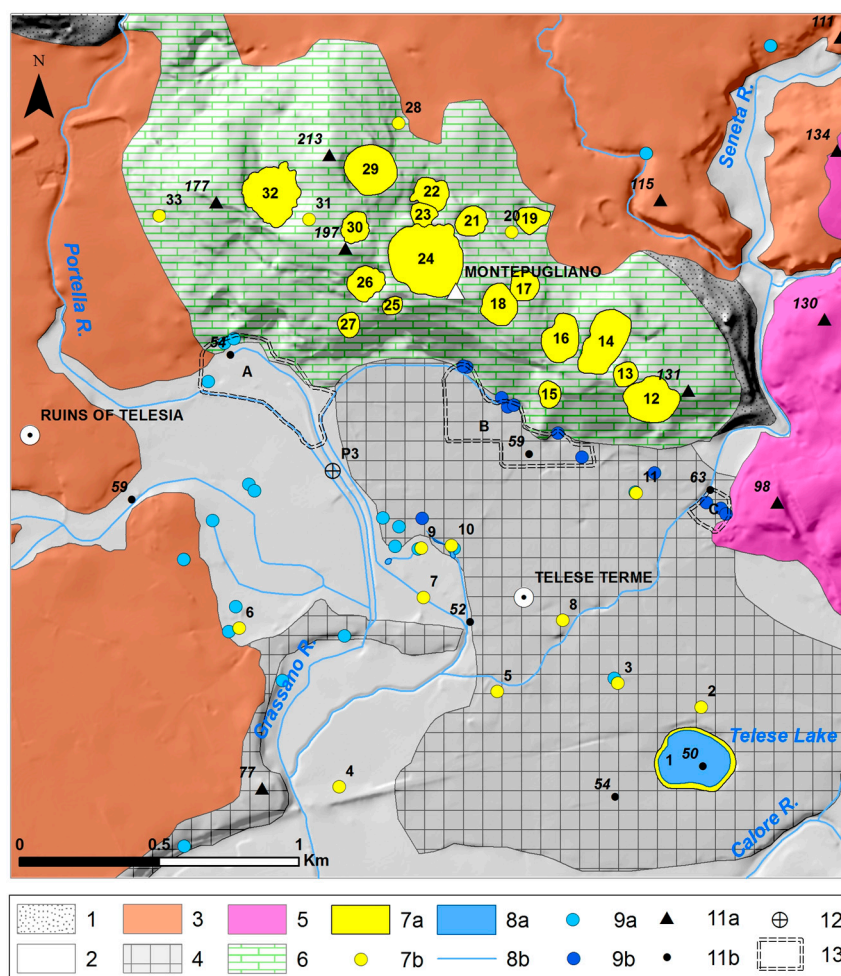


Figure 5. Geological and hydrogeological map of the discharge area of Grassano-Telese springs. (1) Slope deposits; (2) alluvial deposits (Quaternary); (3) Campanian Ignimbrite and pyroclastic deposits; (4) travertine deposits; (5) flysch terrains; (6) limestones and dolostones; (7) main sinkhole (a) and small sinkhole (b); (8) lake (a) and drainage lines (b); (9) cold (a) and sulfurous thermal (b) springs; (11) peak (a) and elevation point (b); (12) borehole; (13) Grassano Park. (A), Terme Minieri Park and (B), Terme Jacobelli Park (C).

South of Montepugliano relief, the Telese plain is constituted by alluvial deposits, which contain travertine sediments and ignimbrite deposits; the latter are dated 39,000 years B.P. and can be associated with the Campanian Ignimbrite [19]. This Quaternary deposit reaches a thickness of tens of meters, and the depth of the below karst substratum is unknown. From a hydrogeological point of view, all these Quaternary deposits can be considered as an aquiclude, thanks also to the presence of the ignimbrite level. Boreholes located in the Telese plain (Figures 4 and 5) have detected artesian conditions of the groundwater.

4. Results

4.1. The Sinkholes of Montepugliano Relief and Telese Plain

A huge number of small to medium-sized closed depressions, or sinkholes, characterizes both the Montepugliano relief and the quaternary deposits of the Telese Plain (Figures 5 and 6).

A very high concentration of karst closed depressions were observed for the carbonate relief of Montepugliano, especially inside the central and western sector; in addition, a main alignment of sinkholes was observed in NW-SE direction, parallel to the Montepugliano ridge direction, where a

probable tectonic line is present. In spite of this, no spatial distribution trend was found for the Telese plain sinkholes.



Figure 6. Drone images (a,b) of Montepugliano sinkholes. Dashed white lines represent the sinkhole rim. Item sinkhole numbers (16, 17, 18, 21, 22, 23, 24, 26, and 32) coincide with those in Figure 5 and Table 2.

A morphometrical description of sinkholes was carried out, and the perimeter, area, circularity index, maximum axis, elevation of the highest point along the sinkhole edge, elevation of the deepest within the sinkhole, and depth are shown in Tables 1 and 2.

Sinkhole perimeter and area are respectively the length of the curve that delimits the sinkhole in plan view and the planimetric surface bounded by the perimeter [20]. Perimeter and area values range between 66.4 and 888.9 m and between 3.2×10^2 and 5.6×10^4 m². The highest values were found for Telese Lake (Figure 5).

Table 1. Main features of sinkholes of the Telese Plain. P_S , sinkhole perimeter; P_{CC} , maximum circumscribed circumference of the sinkhole perimeter; IC, circularity index. Features of sinkholes from 4 to 8 and 11 were masked by buildings, so only their location is known.

Id	Name	Max Diameter (m)	P_S (m)	Area (m ²)	P_{CC} (m)	IC = P_{CC}/P_S	Deepest Point (m a.s.l.)	Highest Point (m a.s.l.)	Depth (m)
1	Telese Lake	291.5	832.0	51,878.9	915.3	1.10	-	54.1	26.0
2	-	27.0	77.5	459.5	84.7	1.09	-	56.7	<5
3	-	54.5	153.3	1799.0	171.2	1.12	-	56.8	-
9	Via Udine sinkhole	25.1	75.5	447.6	79.7	1.06	47.2	53.2	6.0
10	Tre Colori Lake	52.0	138.6	1282.0	163.2	1.18	-	54.2	<5

Table 2. Main features of the sinkholes of the Montepugliano relief. The parameter P_S , P_{CC} , and IC have the same meaning as reported in Table 1.

Id	Name	Max Diameter (m)	P_S (m)	Area (m ²)	P_{CC} (m)	IC = P_{CC}/P_S	Deepest Point (m a.s.l.)	Highest Point (m a.s.l.)	Depth (m)
12	-	204.4	580.7	24,700.8	641.9	1.11	88.2	150.6	62.4
13	-	98.3	283.7	6270.2	308.7	1.09	139.0	157.4	18.4
14	-	258.4	672.3	29,278.8	811.5	1.21	134.3	157.4	23.1
15	-	99.1	282.9	6132.4	311.2	1.10	97.3	140.5	43.3
16	-	179.1	499.6	17,768.1	562.5	1.13	138.9	159.9	21.0
17	-	114.7	345.2	9181.3	362.5	1.05	142.2	171.5	29.3
18	-	153.5	443.3	14,976.4	482.0	1.09	147.6	182.1	34.5
19	-	126.6	349.1	8477.6	397.6	1.14	91.4	117.5	26.1
20	-	-	-	-	-	-	85.0	125.0	40.0
21	Doline Acqua	121.8	358.2	9711.3	382.4	1.07	106.4	164.9	58.5
22	Dolina Mele	145.0	434.6	11,387.6	458.5	1.05	110.7	155.2	44.4
23	Dolina Mele	98.5	300.1	6130.0	319.6	1.06	114.1	167.1	53.0
24	Dolina Grande	290.2	888.9	56,417.0	931.0	1.05	101.3	188.4	87.1
25	-	79.1	221.3	3779.4	248.5	1.12	135.9	175.4	39.6
26	Dolina Falco	141.2	418.4	12,383.6	443.9	1.06	120.3	177.2	56.9
27	-	92.3	269.2	5656.3	290.9	1.08	95.3	128.3	33.0
28	-	-	-	-	-	-	130.0	134.0	4.0
29	Dolina Caprifico	194.4	578.8	26,247.6	610.6	1.05	129.7	206.8	77.1
30	Dolina Rosette	122.6	352.3	8881.7	384.9	1.09	142.0	196.8	54.8
31	-	23.6	66.4	322.9	74.0	1.11	172.4	181.1	8.7
32	Dolina Profonda	239.3	737.9	33,001.7	761.8	1.03	78.1	177.0	98.9
33	-	55.2	164.6	2098.9	176.1	1.07	83.2	112.4	29.2

The circularity index (IC) describes the irregularity of sinkhole planar shape and deviation from a perfect circle [21]; it can be defined as the ratio between the circumference of the circumscribed circle of the sinkhole perimeter and sinkhole perimeter [22]. IC values vary from 1.03 to 1.21; 80% of the sinkholes are sub-circular to sub-elliptical shaped ($IC = 1.05 \div 1.13$).

The maximum axis is the line connecting the two most distant points of the perimeter [20]. The sinkhole's maximum axis is 23.5 to 291.5 m long. Furthermore, 32% of the depressions are characterized by a maximum axis greater than 150 m.

Depth is defined as the difference in elevation between the highest point along the sinkhole edge and the deepest point within the sinkhole [20]. The sinkholes of the Montepugliano relief are the deepest of the study area, with a maximum depth of ≈ 100 m.

Following historical sources [23,24], some sinkholes seemed to originate during the seismic events of 1349 A.D., including the Telese lake, associated with the catastrophic Monte Cassino earthquake of 9 September [25,26]. Subsequent strong earthquakes would probably enlarge the Montepugliano sinkholes [27]. Others sinkholes, located in the eastern sector of the Montepugliano relief, are filled by Campanian Ignimbrite deposits [26].

In the Telese plain, several sinkholes originated recently [28], as that of 7 February, 2002 (Id 9), and during the sixteens (Id 5,6). Based on the shape of the sinkholes, the geological context, and the historical notices, the sinkholes of the Montepugliano relief are typically connected to collapse phenomena; they involve mainly carbonate rocks of the Cretaceous period and can be defined as "collapse sinkholes" [2]. Besides, these sinkholes develop mainly in the unsaturated zone of the aquifer.

The sinkholes of the Telese plain involve mainly deposits of the alluvial plain (travertine, pyroclastic, and alluvial deposits) and can be defined as "cover sinkholes" [29–32]. These sinkholes were filled by groundwater, indicating that they developed mainly in the saturated zone of the aquifer.

The number of sinkholes, especially for the Montepugliano relief, appears anomalous compared with other areas of the Apennines; the mechanism which control their genesis and development appears not well known.

4.2. Groundwater Monitoring

The Grassano-Telese springs are located along the southern side of the Montepugliano relief and can be distinguished into two main groups based on their chemical and physical features: Cold and bicarbonate-calcium large springs, and sulfurous thermal springs. The sulfurous springs are located inside the Telese village, Minieri and Jacobelli Parks (Figures 3 and 5), have a temperature up to 21 °C (Table 3) and overall discharge of a few tens of liters per second. These water springs are naturally enriched in H₂S and CO₂ [15] and are used for thermal purposes and bottling. Some further sulfurous springs are scattered in the Telese plain such as that of Tre Colori (Figure 5; Table 3).

The Grassano springs are located on the western side of Telese village; they are characterized by several outlets discharging directly by the rock of the Montepugliano relief, with an elevation of 54 m a.s.l.; other springs are located along the Rio Grassano bed (Figure 5). Spring waters have a temperature of 11 °C, discharge of several thousands of liters per second, presence of CO₂, and absence of H₂S.

The Grassano springs are partially used for irrigation, only a minimum amount is tapped as drinkable water; the largest amount flows downstream toward the Calore river. Between these two main groups, some other minor springs appear to have geochemical intermediate characteristics [12], with a temperature of 14 °C, and minor concentrations of H₂S and CO₂ compared to the Telese group (Table 3).

Discharge measurements of the Grassano springs have been carried out in correspondence with a local bridge, which crosses the river downstream of all spring outlets (Figure 3c); other field measurements were carried out in correspondence with spring outlets.

Table 3. Chemical and physical characteristics of spring and well waters. Type: A, sulfurous thermal spring; B, cold spring. Location: 1, Jacobelli Park; 2, Minieri Park; 3, Grassano Park; 4, other. S. Stefano, Pera, Goccioloni, and Bouvette are tapped by wells.

Spring Name	Type and Location	pH	T (°C)	E.C. (µS/cm)	Na ⁺ (mg/L)	K ⁺ (mg/L)	Ca ²⁺ (mg/L)	Mg ²⁺ (mg/L)	NH ₄ ⁺ (mg/L)	Cl ⁻ (mg/L)	HCO ₃ ⁻ (mg/L)	SO ₄ ²⁻ (mg/L)	NO ₃ ⁻ (mg/L)	CO ₂ (mg/L)	H ₂ S (mg/L)
Jacobelli ¹	A 1	6.0	16.9	1670	-	-	-	-	-	-	-	-	-	-	-
S. Stefano ^{2a}	A 4	6.3	20.5	1838	59.8	8.4	253.3	59.48	0.45	78.9	1393.0	12.98	3.0	-	3.3
S. Stefano ^{2c}	A 4	6.2	18.5	1669	57.4	9.4	356	52.7	<0.02	79.3	1324.0	31.5	1.0	638.0	10.6
S. Stefano ⁴	A 4	6.5	20.0	2028	119.8	21.1	390.8	57.1	-	158.1	1526.1	25.0	-	786	15.3
Pera ^{2a}	A 2	6.3	20.7	2440	115.3	14.6	410.0	86.0	-	105.6	1617.0	24.5	-	-	2.8
Goccioloni ^{2b}	A 2	6.3	19.5	2187	91.0	16.0	628	82.0	<0.02	121.0	2049.0	18.0	3.0	1268.0	9.8
Diana ^{2a}	A 2	6.3	21.3	2650	122.0	19.0	359.0	151.0	-	172.0	1891.0	41.0	-	-	11.0
Diana ^{2c}	A 2	6.0	20.1	2518	126.0	18.4	473.0	79.5	<0.02	181.0	1886.0	61.4	1.0	672.0	12.7
Bouvette ^{2b}	A 2	6.3	19.3	2264	85.0	14.6	539.0	71.0	0.2	131.0	1833.0	27.3	2.0	988.0	8.9
Bouvette ⁴	A 2	6.4	21.0	2381	110.4	16.0	358.7	118.0	-	192.8	1637.2	28.3	-	716.0	18.3
Lucia ³	A 2	6.2	20.1	2567	100.7	15.0	423.6	68.4	-	152.1	1617.6	35.8	0.3	-	-
Tre Colori ¹	A 4	6.0	16.2	1830	-	-	-	-	-	-	-	-	-	-	-
Cerro ⁴	B 2	6.3	14.0	1340	16.1	3.5	272.5	63.4	-	56.0	976.3	26.4	-	400.0	2.0
Grassano ¹	B 3	6.4	11.9	1110	-	-	-	-	-	-	-	-	-	-	-
Grassano ^{2a}	B 3	7.0	-	761	15.2	2.2	181.7	28.2	-	28.6	701.3	8.5	1.7	-	-
Grassano ⁴	B 3	6.5	11.0	818	7.6	2.2	160.3	23.1	-	30.1	568.1	6.2	-	116.0	0.0

¹ Data acquired using a multiparameter water quality meter, between January and February 2019; ² Impresa Minieri S.p.A. relative to years ^a 2000, ^b 2017, and ^c 2018; ³ Harabaglia et al. (2002); ⁴ Corniello and De Riso (1986).

Temperature values were about 11.6 °C (range 11.4–11.8 °C) and electrical conductivity was around 1150 $\mu\text{S}/\text{cm}$ (range 1130–1180 $\mu\text{S}/\text{cm}$; Figure 7); these parameters appeared almost constant through the hydrological year, pointing out a strong control of the aquifer in which large water volumes are involved.

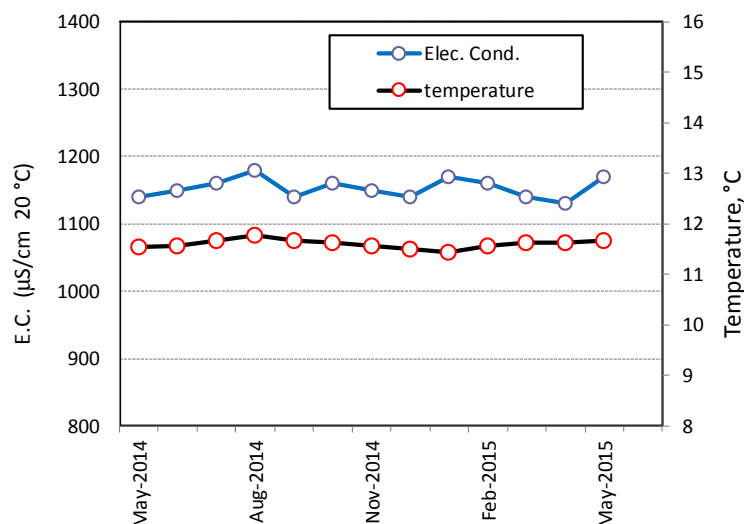


Figure 7. Temperature and electrical conductivity measured in the Grassano river, just below spring outlets; monthly measurements from May 2014 to May 2015 (modified from Fiorillo et al. [33]).

During the 2014–2018 period, spring discharge range between the minimum of 2.5 m^3/s during the 2017 drought to a maximum value greater than 6 m^3/s . Figure 8 shows the results of discharge measurements together with ^{222}Rn activity, which were carried out for two distinct spring outlets of the Grassano river in the period from May 2014 to May 2015. The activity of ^{222}Rn increases according to spring discharge, and decreases following the discharge as well; thus, the maximum and minimum activity of ^{222}Rn occur during high flow and low flow conditions, respectively, as also found in other springs of the Apennine [4].

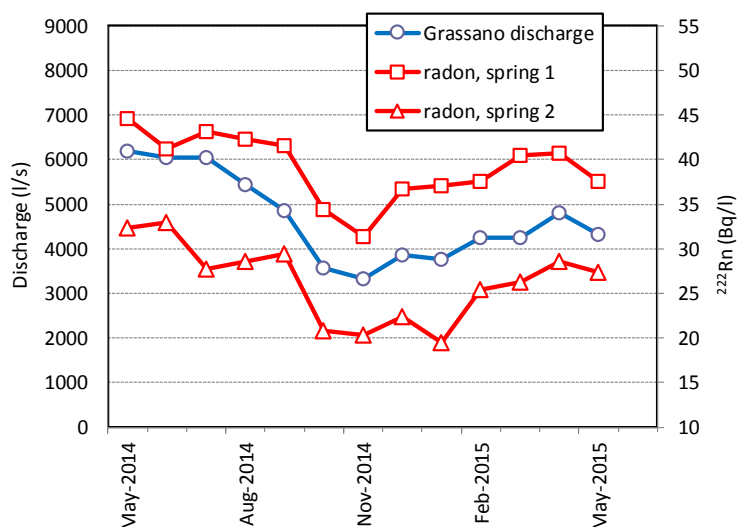


Figure 8. Radon (^{222}Rn) activity measured in two distinct spring outlets (1 and 2) of the Grassano group, and overall discharge of the Grassano; monthly measurements from May 2014 to May 2015.

The hydraulic head of the groundwater was detected in some boreholes located in Figures 4 and 5, and is shown in Figure 9. These measurements allow the reconstruction of the water table in

the karst system feeding the Grassano springs, as shown in Figure 9a. As can be seen, the slope of the water table is very low; 10 km upstream of the spring outlets, the hydraulic head is 65 m a.s.l., indicating a slope of the water table of 0.0011. Downstream of the spring outlets, the hydraulic head measured in several boreholes points out artesian conditions, with hydraulic head higher than the spring elevation; in particular, a hydraulic head of 55 m a.s.l. was detected in a group of boreholes located 1 km downstream of the spring outlets.

To reach the spring outlet, groundwater has to syphon below the flysch sequences located between the Matese massif and the Montepugliano reliefs. Looking at the map of Figure 4, a groundwater connection could exist through Mt. Monaco, Mt. Acero, and Montepugliano reliefs, but it seems to not fully explain the high discharge observed at Grassano springs; as before described, the main recharge area of these springs involves a wider area of the Matese massif.

4.3. Groundwater Modeling with Modflow Numerical Code

The hydraulic features were further investigated proposing a hydraulic model in the MODFLOW environment, describing the upwelling flux for the Rio Grassano spring. The aim of the model is to provide a possible scenario of groundwater circulation affected by ascendant flow in which the Montepugliano relief constitutes the discharge zone of a wide karst area (eastern side of Matese massif).

The hydrogeological model was built using PROCESSING MODFLOW creating a grid with cell size 100×100 m, with length 12 km, between Mt. Monaco and Telese plain (Figures 4 and 9b); a constant thickness/depth has been assumed for the karst aquifer, considering values up to 2000 m. The water flow occurs inside this aquifer, which is below limited by the no-karstification zone, whereas flysch sequences are no-flow zone.

The model considers an unconfined karst aquifer in a steady-state condition (Figure 9a); the groundwater flow comes from the left side, where the recharge area (Matese massif) is located. The alluvial complex of the Telese plain has been considered as an aquitard, with a hydraulic conductivity one order of magnitude lesser than karst medium. The hydraulic head has been deducted by piezometer upstream of spring outlets (Figure 9a). Downstream of the spring outlets, the hydraulic head has been inferred by the model and compared with that observed in the Telese plain (Figure 9a). The Montepugliano relief appears as a drain, where all flow lines converge and originate the spring outlets. The model was run for different values of the hydraulic conductivity of karst medium, to obtain a hydraulic head that in correspondence with the Montepugliano relief is coherent with spring elevation. Thus, the elevation of the Grassano springs has been used to calibrate the model and has allowed to fix the hydraulic conductivity of karst medium. Figure 10 shows that a value of $K = 0.001$ m/s provides the best result; this value is in line with the estimated hydraulic conductivity found in other karst areas of the Apennines [34]; as a consequence, a value of $K = 0.0001$ m/s [35] was used for the aquitard (alluvial, pyroclastic, and travertine deposits of the Telese plain).

The flow net has been provided by MODPATH and highlights the upwelling phenomenon in correspondence of the Montepugliano relief, independently from the depth of the karst aquifer. Of course, the model also shows that the groundwater flow lines come mainly from the left side (eastern zone of Matese massif), which is the main recharge area of the Grassano springs catchment.

In the Telese plain, the model also highlights how the groundwater could have artesian behavior, as effectively found in several boreholes locally drilled.

It has to be specified, that the aquifer cannot be considered an isotropic medium in terms of hydraulic conductivity, as groundwater mainly flows into fractures and karst conduits; this simplification of the model, only provides an overview of the groundwater flow, but explains many hydrological processes locally observed.

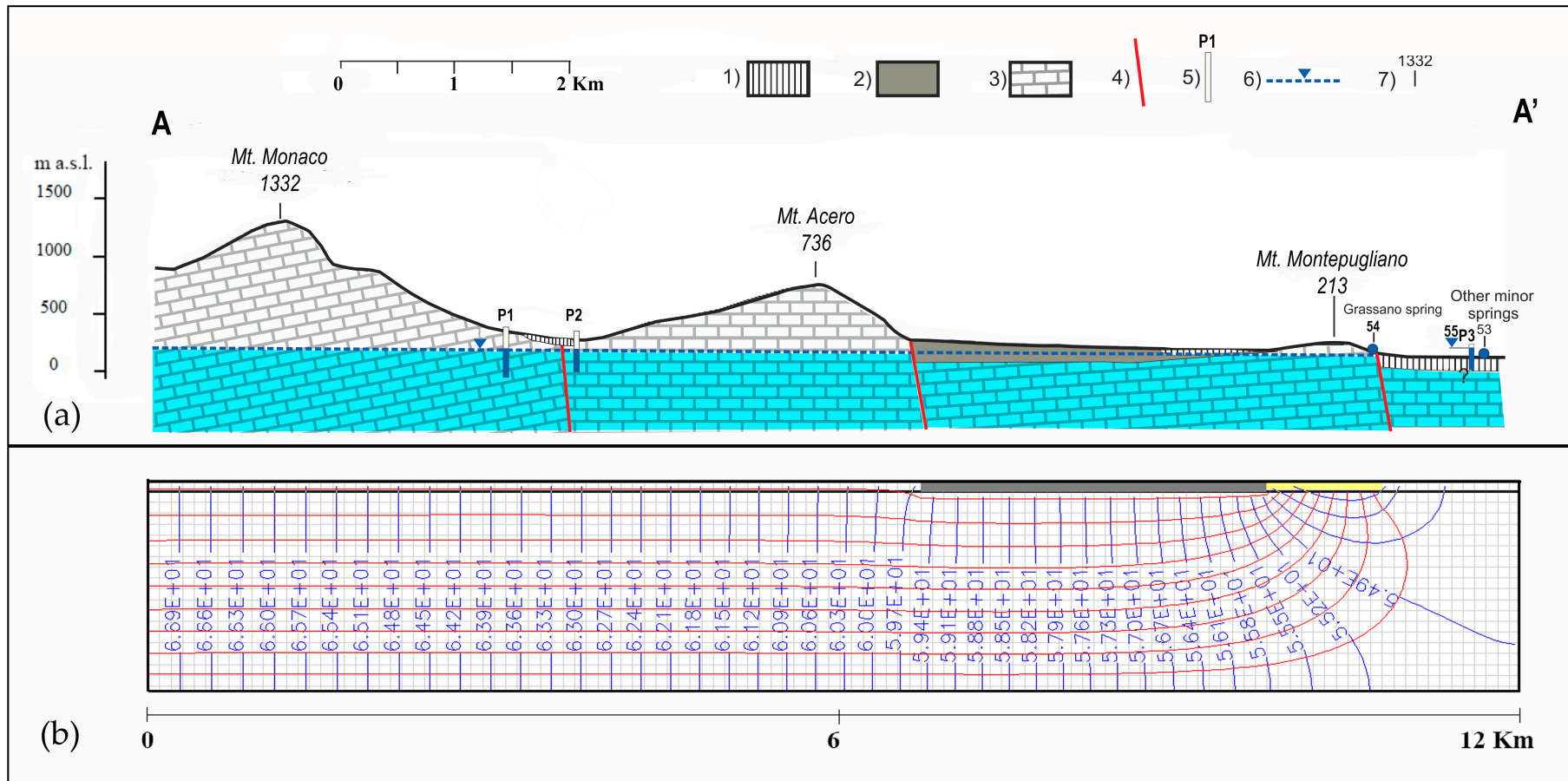


Figure 9. (a) Hydrogeological cross-section (trace AA' in Figure 4). The water table has been drawn by piezometers P1 and P2. Artesian conditions are detected in the Telese plain by borehole P3. (1) Aquitard (alluvial, pyroclastic, and travertine complex); (2) aquiclude (flysch sequences); (3) karst aquifer (carbonate sequences); (4) fault; (5) borehole; (6) hydraulic head; (7) elevation point. (b) MODFLOW numerical code simulation along the cross-section AA'. Flow net highlights the upwelling phenomenon in correspondence with the Montepugliano relief; numbers show the hydraulic head of each equipotential line (m a.s.l.).

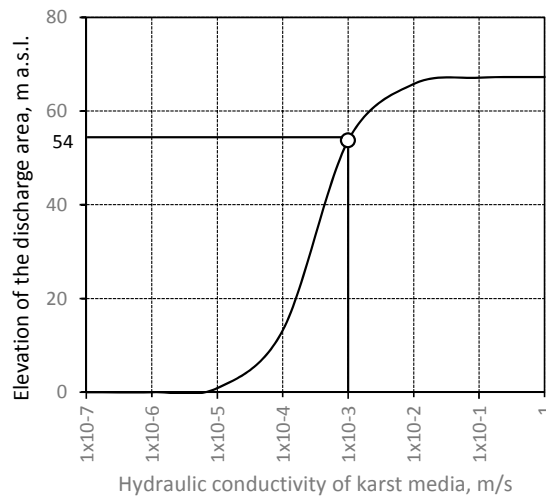


Figure 10. Relationship between hydraulic conductivity of karst media and discharge area elevation; The Rio Grassano elevation (54 m a.s.l.) was obtained considering hydraulic conductivity $K = 0.001$ m/s.

5. Discussion

In the karst area of Teleso plain are located both large cold springs and sulfurous thermal springs and their main geochemical features have been shown in Table 3. In the Schoeller diagram (Figure 11) the different springs show similar ratios between each component, but the anion and cation concentrations increase from cold waters (Grassano springs) to sulfurous thermal waters (Teleso springs), and thus from the western to the eastern side of southern boundary of the Montepugliano relief (Figure 5). Similarly, the temperature of the waters and H_2S concentrations increase toward the East.

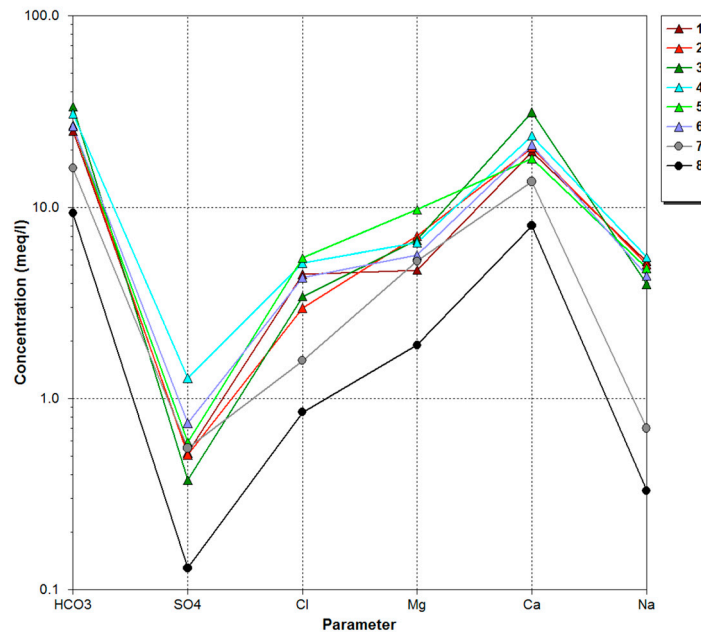


Figure 11. Schoeller diagram of spring and well waters. Triangles are relative to sulfurous thermal waters; circles are relative to cold waters. 1, S. Stefano spring (Corniello and De Riso, 1986); 2, Pera spring (Impresa Minieri S.p.A, 2000); 3, Goccioloni well (Impresa Minieri S.p.A, 2017); 4, Diana well (Impresa Minieri S.p.A., 2018); 5, Bouvette well (Corniello and De Riso, 1986); 6, S. Lucia spring (Harabaglia et al., 2002); 7, Cerro spring (Corniello and De Riso, 1986); 8, Grassano spring (Corniello and De Riso, 1986).

The hydrogeological scheme of Figure 9a and the relative simulated groundwater flow path (Figure 9b) are related to the Grassano (cold) springs. Conversely, the sulfurous thermal springs have to be ascribable to a different karst aquifer, although they can partially be diluted and cooled by the waters of the Grassano springs aquifer just before emerging. More in detail, with respect to Grassano springs, these sulfurous thermal springs originate from a greater depth and come from a different zone of the Matese massif; their recharge area could be located in eastern side of the Matese massif, and would need further surveys to be ascertained.

The Montepugliano relief can be considered the discharge area of all springs, where the drainage of different recharge zones converges locally.

The upwelling phenomenon occurs for both types of waters (cold and sulfurous thermal springs) and has been highlighted using MODFLOW tools for the Grassano (cold) springs.

The focus of the groundwater model is to provide only a qualitative overview of the groundwater path affecting the Grassano springs; in particular, the groundwater model is not focused on water budget assessment, and the recharge volumes involved in the Grassano springs need further in-depth analysis, as 3D models.

The phenomenon of the upwelling flow in the Telese area explains different types of evidences. The amazing density of sinkholes on the Montepugliano relief is in line with ascendant flow conditions: The flow lines terminate within the Montepugliano relief, transporting in solution CO₂ and H₂S from the depth. Therefore, the geomorphological processes that have led to the formation of sinkholes are of a hypogenic type [36,37], connected with the ascendant flow of groundwater. In these environments, as known, the development of voids is intense at the phreatic surface, due to the need for oxygen to oxidize sulfur [36,38]. In addition, the Montepugliano relief should be affected by a dense network of caves, only partially identified [15].

Thus, similarly to other springs of the Apennines, such as that of the Frasassi caves [39], the deep origin of the fluid [40] has caused the speleogenesis of the Montepugliano relief.

The sinkholes of the Telese plain also can be connected to local hydraulic conditions where the alluvial complex deposits constitute an aquitard which causes confined conditions of the aquifer. The groundwater artesian conditions detected in the Telese plain can be explained by the upwelling flow, which locally is confined by the aquitard role of the alluvial deposits of the plain. Thus, also in this area, CO₂ and H₂S coming from the ascendant groundwater appear to be the main factors controlling the dissolution processes and the underground void genesis especially in the travertine deposits.

The other important consequence of the upwelling flow appears to be the constancy of physical characteristics of the water over time, such as temperature and electrical conductivity, as observed also for the Serino springs [4]. Besides, similarly to Serino springs, the radon activity varies, according to the fact that during the periods of high flow, the greater velocity of ascendant groundwater favors greater radon activity; vice versa, during periods of low flow, the slower ascendant groundwater favors lower radon activity [4].

As recognized in many karst aquifers of southern Italy, the water table has a gentle slope, with values lower than 1% [41]. This characteristic appears to be an important diagnostic feature to recognize the upwelling flow occurring in the discharge area. In fact, this condition favors a deep circulation, with flow lines initially descending (recharge zone), then converging toward springs (discharge zone), where they concentrate with a kind of flow typically ascendant (Figure 1); the horizontal component of the flow is prevalent in the median zone of the groundwater flow path. The case of Grassano springs, associated to the general sketch case of Figure 1b, has been detailed in Figure 12, where some hydraulic features highlight the upwelling phenomenon in the discharge area: (i) As observed in the field, the hydraulic head downstream of the spring outlets can be higher than spring elevation, (ii) upstream of the spring outlets, a gentle slope of the water table would not support the high discharge measured at the spring outlets, which need a vertical component of the groundwater path.

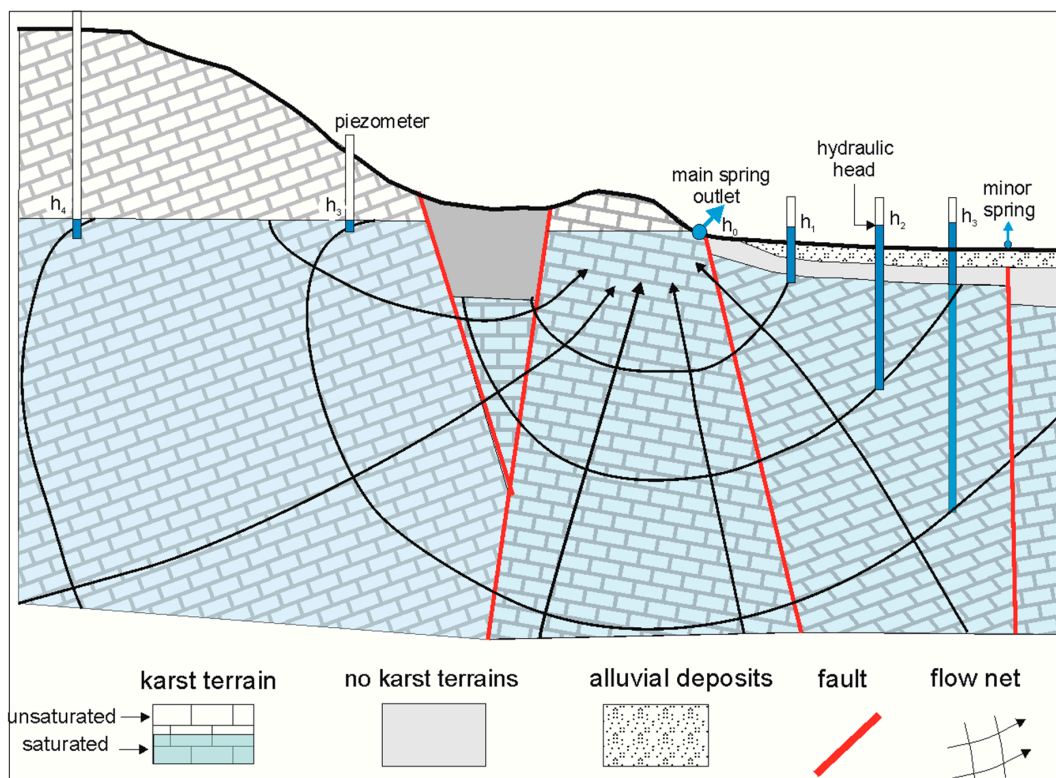


Figure 12. General sketch of the groundwater path (detail of Figure 1b), with flow net deduced from hydraulic heads detected into piezometers located upstream and downstream of the main spring outlet; recharge area is located on the left side.

The flow lines of Figure 1 have been plotted considering an isotropic media, simply to provide a sketch of the groundwater flow. As is well known, during the time conduits network development leads to flow hierarchization [42], which has a strong control on the groundwater path. The ascendant flow feeding springs is probably the cause of sub-vertical conduit formation that can typically end in outlet springs [4] as in the case of the Vauclisian type springs. Besides, tectonic displacements along the faults, which split karst terrain by less permeable deposits favor sub-vertical conduit formations [43].

Because of the local hydraulic conditions, the Montepugliano relief can be considered as a “drain”, where a deep and wide groundwater circulation locally converge providing a general upwelling flow; the spring front of the Rio Grassano appears to be the overflow of this powerful upwelling flow, driven by conduits and fracture networks.

6. Conclusions

The research focuses on the peculiarity of the hydraulic aspects of the Teleso karst area (southern Italy), characterized by a wide and complex groundwater circulation.

Two main kind of spring outlets characterize this karst area: Sulfurous thermal and cold large springs. The springs are located along the foot of a karst relief (Montepugliano) which constitutes the drainage of a large portion of the Matese massif.

The amazing concentration of sinkholes and the water’s chemical and physical features seem to ascertain the hydraulic phenomenon of upwelling, further proved by piezometer monitoring. The flow net of the karst aquifer feeding the Grassano springs has been drawn using MODFLOW tools. The groundwater flow 2D model can be considered a simple tool to understand groundwater circulation affecting the Rio Grassano karst aquifer, providing a possible scenario of groundwater behavior, it is not certain whether the model assesses the recharge water amount involved in discharge zones, which requires a tridimensional model.

The sulfurous thermal springs of the Teleso Plain are also likely to be associated with the upwelling phenomenon, but the recharge area and the relative aquifer should be different from that of the Grassano springs. Under such a hypothesis, the Montepugliano relief constitutes the same discharge area for both the spring groups, draining aquifers located in different zone of the Matese massif.

Finally, the assessment of the water circulation in the karst aquifer allows us to design an accurate strategic plan for the realization of the tapping work, in their maintenance and for the definition of the protection area of the springs.

Author Contributions: F.F. wrote the text and coordinated the research with L.E. G.L. analyzed remotely sensed data for sinkhole characterization and provided photos. M.P. designed and validated the groundwater model of the karst aquifer, exploiting piezometer data. V.C. carried out in situ measurements related to spring discharge, water chemical–physical features, and radon activity. G.T. analyzed data series related to spring water.

Funding: This research has been partially supported by E.ON Climate & Renewables Italia s.r.l.

Acknowledgments: Authors are grateful to Alto Calore Servizi S.p.A. for precious help providing piezometer data detected by boreholes. Thanks to Elda Vecchi of Minieri Park for chemical and physical data on sulfurous thermal springs, Pompilio Colella of the Grassano Park for his availability in monitoring the spring discharge. Thanks also to Domenico Cicchella, University of Sannio, for his support during the radon activity measurements.

Conflicts of Interest: The authors declare no conflict of interest.

References

- White, W.B. *Geomorphology and Hydrology of Karst Terrains*; Oxford University Press: Oxford, NY, USA, 1988; p. 464.
- Ford, D.; Williams, P. *Karst Hydrogeology and Geomorphology*; Wiley: Chichester, UK, 2007; p. 562.
- Stevanovic, Z.; Kresic, N. *Groundwater Hydrology of Springs*; Butterworth Heinemann-Elsevier: Oxford, UK, 2009; p. 592.
- Fiorillo, F.; Esposito, L.; Testa, G.; Ciarcia, S.; Pagnozzi, M. The Upwelling Water Flux Feeding Springs: Hydrogeological and Hydraulic Features. *Water* **2018**, *10*, 501. [[CrossRef](#)]
- Hubbert, M.K. The theory of groundwater motion. *J. Geol.* **1940**, *48*, 785–944. [[CrossRef](#)]
- Toth, J. A theoretical analyses groundwater flow in small drainage basins. *J. Geophys. Res.* **1963**, *68*, 4795–4812. [[CrossRef](#)]
- Domenico, P.A.; Schwartz, F.W. *Physical and Chemical Hydrogeology*; John Wiley & Sons: Singapore, 1990; p. 824.
- Chiang, W.H.; Kinzelbach, W. *Processing MODFLOW. A Simulation System for Modelling Groundwater Flow and Pollution*; Springer: Hamburg, Germany, 1998; p. 342.
- Chiang, W.H. *3D-Groundwater Modeling with PMWIN: A Simulation System for Modeling Groundwater Flow and Transport Processes*, 2nd ed.; Springer: Berlin, Germany, 2005; p. 397.
- Fioreze, M.; Mancuso, M.A. MODFLOW and MODPATH for hydrodynamic simulation of porous media in horizontal subsurface flow constructed wetlands: A tool for design criteria. *Ecol. Eng.* **2019**, *130*, 45–52. [[CrossRef](#)]
- Jankovic, I.; Maghrebi, M.; Fiori, A.; Dagan, G. When good statistical models of aquifer heterogeneity go right: The impact of aquifer permeability structures on 3D flow and transport. *Adv. Water Resour.* **2017**, *100*, 199–211. [[CrossRef](#)]
- Gauthier, V. L'Idrografia dell'Agro Telesino. *Boll. Soc. Nat. Napoli* **1910**, *24*, 9–17. (In Italian)
- Civita, M. Valutazione analitica delle riserve in acque sotterranee alimentanti alcune tra le principali sorgenti del massiccio del Matese (Italia meridionale). *Mem. Soc. Nat. Napoli* **1969**, *78*, 133–163. (In Italian)
- Celico, P. Schema idrogeologico dell'Appennino carbonatico centro-meridionale. *Memorie e Note Istituto di Geologia Applicata* **1978**, *14*, 1–43. (In Italian)
- Corniello, A.; De Riso, R. Idrogeologia e idrochimica delle sorgenti dell'Agro Telesino. *Geologia applicata e Idrogeologia* **1986**, *21*, 53–84. (In Italian)
- Celico, P.; Celico, F.; Cacciuni, A. Experimental hydrogeological cartography of the Monti del Matese and Monte Totila districts (Campania-Molise, Italy). *Memorie Descrittive Carta Geologica d'Italia* **2008**, *LXXXI*, 115–136. (In Italian)

17. Fiorillo, F.; Pagnozzi, M. Recharge process of Matese karst massif (southern Italy). *Environ. Earth Sci.* **2015**, *74*, 7557–7570. [[CrossRef](#)]
18. Robustini, P.; Corrado, S.; Di Bucci, D.; Calabro', R.A.; Tornaghi, M. Comparison between contractional deformation styles in the Matese Mountain: Implications for shortening rates in the Apennines. *Boll. Soc. Geol. Ital.* **2003**, *122*, 295–306.
19. De Vivo, B.; Rolandi, G.; Gans, P.B.; Calvert, A.; Bohrson, W.A.; Spera, F.J.; Belkin, H.E. New constraints on the pyroclastic eruptive history of the Campanian volcanic Plain (Italy). *Mineral. Petrol.* **2001**, *73*, 47–65. [[CrossRef](#)]
20. Basso, A.; Bruno, E.; Parise, M.; Pepe, M. Morphometric analysis of sinkholes in a karst coastal area of the southern Apulia (Italy). *Environ. Earth Sci.* **2013**, *70*, 2545–2559. [[CrossRef](#)]
21. Šegina, E.; Benac, Č.; Rubinić, J.; Knez, M. Morphometric analyses of dolines: The problem of delineation and calculation of basic parameters. *Acta Carsol.* **2018**, *47*, 23–33. [[CrossRef](#)]
22. Bondesan, A.; Meneghel, M.; Sauro, U. Morphometric analysis of dolines. *Int. J. Speleol.* **1992**, *21*, 1–55. [[CrossRef](#)]
23. Rossi, D. Sulle acque minerali di Telesse e sullo Stabilimento dei Bagni qui vi costruito. *Ann. Civ. Regno delle due Sicilie* **1857**, *61*. (In Italian)
24. Ricciardi, L. *Telesse: Ricordi e speranze*; Tipografia Nazzareno Borrelli: Benevento, Italy, 1927.
25. Del Prete, S.; De Riso, R.; Santo, A. Primo contributo sui sinkholes di origine naturale in Campania. In Proceedings of the Atti Conv. "Stato dell'arte sullo studio dei fenomeni di sinkholes e ruolo delle amministrazioni statali locali nel governo del territorio", Rome, Italy, 20–21 May 2004; APAT: Rome, Italy; pp. 361–376.
26. Del Prete, S.; Di Crescenzo, G.; Santo, A. I sinkhole dell'appennino campano: Stato delle conoscenze. In Proceedings of the Atti 2° Workshop Internazionale sui sinkhole, I sinkhole. Gli sprofondamenti catastrofici nell'ambiente naturale ed in quello antropizzato, Rome, Italy, 3–4 December 2009; ISPRA-Servizio Geologico d'Italia: Rome, Italy; pp. 283–298.
27. Porfido, S.; Esposito, E.; Vittori, E.; Tranfaglia, G.; Micheti, A.M.; Blumetti, M.; Ferrel, L.; Guerrieri, L.; Serva, L. Areal distribution of round effects induced by strong earthquakes in southern Apennines (Italy). *Surv. Geophys.* **2002**, *23*, 529–562. [[CrossRef](#)]
28. Calcaterra, D.; Esposito, A.; Fuschini, V.; Galluccio, F.; Giulivo, I.; Nardò, S.; Russo, F.; Terranova, C. L'utilizzo della tecnica Psinsar™ per l'individuazione ed il monitoraggio di sinkholes in aree urbanizzate della Campania: I casi di Telesse Terme (BN) e Sarno (SA). In 2° Workshop "I sinkholes. Gli sprofondamenti catastrofici nell'ambiente naturale ed in quello antropizzato"; ISPRA-Servizio Geologico d'Italia: Rome, Italy; pp. 931–948.
29. Tharp, T.M. The engineering geology and hydrogeology of karst terraines. In Proceedings of the 6th Multidisciplinary Conference on Sinkholes and the Engineering and the Environmental Impacts of Karst, Springfield, MO, USA, 6–9 April 1997; pp. 29–36.
30. Nisio, S.; Graciotti, R.; Vita, L. I fenomeni di sinkholes in Italia: Terminologia, meccanismi genetici e problematiche aperte. In Atti Con. Stato dell'arte sullo studio dei fenomeni di sinkholes e ruolo delle amministrazioni statali e locali nel governo del territorio; APAT: Rome, Italy, 2004; pp. 557–571.
31. Waltham, T.; Bell, F.; Culshaw, M. *Sinkholes and Subsidence: Karst and Cavernous Rock in Engineering and Construction*; Springer: Berlin/Heidelberg, Germany, 2005; p. 382.
32. De Waele, J.; Gutiérrez, F.; Parise, M.; Plan, L. Geomorphology and natural hazards in karst areas: A review. *Geomorphology* **2011**, *134*, 1–8. [[CrossRef](#)]
33. Fiorillo, F.; Esposito, L.; Pagnozzi, M.; Ciarcia, S.; Testa, G. Karst springs of Apennines typified by upwelling flux "Sorgenti carsiche dell'Appennino interessate da flusso ascendente". *Acque Sotterranee—Italian J. Groundwater* **2018**, *7*, 21–30.
34. Lancia, M.; Saroli, M.; Petitta, M. A double scale methodology to investigate flow in karst fractured media via numerical analysis: The Cassino plain case study (Central Apennine, Italy). *Geofluids* **2018**, 2937105. [[CrossRef](#)]
35. Civita, M. *Idrogeologia applicata e ambientale*; Casa Editrice Ambrosiana: Milano, Italy, 2009; p. 794.
36. Palmer, A.N. Sulfuric acid caves: Morphology and evolution. Treatise on Geomorphology. *Karst Geomorphol.* **2013**, *6*, 241–257.

37. Palmer, A.N. Sulfuric acid vs. epigenic carbonic acid in cave origin and morphology. In Proceedings of the Deep Karst: Origins, Resources, and Management of Hypogene Karst, Carlsbad, NM, USA, 11–14 April 2016; pp. 7–15.
38. Frumkin, A.; Zaidner, Y.; Na'aman, I.; Tsatskin, A.; Porat, N.; Vulfson, L. Sagging and collapse sinkholes over hypogenic hydrothermal karst in carbonate terrain. *Geomorphology* **2015**, *229*, 45–57. [[CrossRef](#)]
39. Galdenzi, S.; Cochioni, M.; Morichetti, L.; Amici, V.; Scuri, S. Sulfidic ground-water chemistry in the Frasassi caves, Italy. *J. Cave Karst Stud.* **2008**, *70*, 94–107.
40. Harabaglia, P.; Mongelli, G.; Paternoster, M. A Geochemical Survey of the Telesse Hypothermal Springs, Southern Italy: Sulfate Anomalies Induced by Crustal Deformation. *Environ. Geosci.* **2002**, *9*, 89–101. [[CrossRef](#)]
41. Fiorillo, F.; Petitta, M.; Preziosi, E.; Rusi, S.; Esposito, L.; Tallini, M. Long-term trend and fluctuations of karst spring discharge in a Mediterranean area (central-southern Italy). *Environ. Earth Sci.* **2015**, *74*, 153–172. [[CrossRef](#)]
42. Király, L. Karstification and groundwater flow. In *Evolution of Karst: From Prekarst to Cessation*; Gabrovšek, F., Ed.; ZRC Publishing: Ljubljana, Slovenia, 2002; pp. 155–190.
43. Palmer, A.N.; Audra, P. Patterns of caves. In *Encyclopedia of Cave and Karst Science Fitzroy Dear-Born*; Gunn, J., Ed.; Taylor and Francis Group: London, UK, 2004; pp. 573–574.



© 2019 by the authors. Licensee MDPI, Basel, Switzerland. This article is an open access article distributed under the terms and conditions of the Creative Commons Attribution (CC BY) license (<http://creativecommons.org/licenses/by/4.0/>).